ELSEVIER

The Spine Journal 5 (2005) 297–309

THE SPINE JOURNAL

Influence of spine morphology on intervertebral disc loads and stresses in asymptomatic adults: implications for the ideal spine

Tony S. Keller, PhD[a,*], Christopher J. Colloca, DC[b], Deed E. Harrison, DC[c], Donald D. Harrison, DC, PhD[d], Tadeusz J. Janik, PhD[e]

[a]*Department of Mechanical Engineering, Department of Orthopaedics and Rehabilitation, University of Vermont, 33 Cochester Avenue, Burlington, VT 05405-0156, USA*

[b]*Department of Kinesiology, Arizona State University, Tempe, AZ 85287, USA; State of the Art Chiropractic Center, P.C., 11011 S. 48th Street, Phoenix, AZ, 85044, USA*

[c]*Ruby Mountain Chiropractic Center, 123 2nd Street, Elko, NV 89801, USA*

[d]*Biomechanics Laboratory, Université du Québec a Trois-Rivières, 3351 Boulevard des Forges, CP 500, Québec, G9A 5H7, Canada*

[e]*CompMath R/C, Huntsville, AL 35806, USA*

Received 3 March 2004; accepted 29 October 2004

Abstract

BACKGROUND CONTEXT: Sagittal profiles of the spine have been hypothesized to influence spinal coupling and loads on spinal tissues.

PURPOSE: To assess the relationship between thoracolumbar spine sagittal morphology and intervertebral disc loads and stresses.

STUDY DESIGN: A cross-sectional study evaluating sagittal X-ray geometry and postural loading in asymptomatic men and women.

PATIENT SAMPLE: Sixty-seven young and asymptomatic subjects (chiropractic students) formed the study group.

OUTCOME MEASURES: Morphological data derived from radiographs (anatomic angles and sagittal balance parameters) and biomechanical parameters (intervertebral disc loads and stresses) derived from a postural loading model.

METHODS: An anatomically accurate, sagittal plane, upright posture, quadrilateral element model of the anterior spinal column (C2-S1) was created by digitizing lateral full-spine X-rays of 67 human subjects (51 males, 16 females). Morphological measurements of sagittal curvature and balance were compared with intervertebral disc loads and stresses obtained using a quadrilateral element postural loading model.

RESULTS: In this young (mean 26.7, SD 4.8 years), asymptomatic male and female population, the neutral posture spine was characterized by an average thoracic angle (T1-T12)=+43.7° (SD 11.4°), lumbar angle (T12-S1)=−63.2° (SD 10.0°), and pelvic angle=+49.4° (SD 9.9°). Sagittal curvatures exhibited relatively broad frequency distributions, with the pelvic angle showing the least variance and the thoracic angle showing the greatest variance. Sagittal balance parameters, C7-S1 and T1-T12, showed the best average vertical alignment (5.3 mm and −0.04 mm, respectively). Anterior and posterior disc postural loads were balanced at T8-T9 and showed the greatest difference at L5-S1. Disc compressive stresses were greatest in the mid-thoracic region of the spine, whereas shear stresses were highest at L5-S1. Significant linear correlations ($p<.001$) were found between a number of biomechanical and morphological parameters. Notably, thoracic shear stresses and compressive stresses were correlated to T1-T12 and T4-hip axis (HA) sagittal balance, respectively, but not to sagittal angles. Lumbar shear stresses and body weight (BW) normalized shear

FDA device/drug status: not applicable.

Support in whole or in part was received from Chiropractic Biophysics Nonprofit, Inc. and The Foundation for the Advancement of Chiropractic Education, nonprofit organizations. Nothing of value received from a commercial entity related to this research.

This study was presented, in part, at the 30th Annual Meeting of the International Society for the Study of the Lumbar Spine, Vancouver, British Columbia, Canada, May 13–17, 2003.

* Corresponding author. The University of Vermont, Department of Mechanical Engineering, 119C Votey Building, Burlington, VT 05405-0156. Tel.: (802) 656-1936; Fax: (802) 656-4441.

E-mail address: keller@emba.uvm.edu (T.S. Keller)

1529-9430/05/$ – see front matter © 2005 Elsevier Inc. All rights reserved.

doi:10.1016/j.spinee.2004.10.050

loads were correlated with T12-S1 balance, lumbar angle, and sacral angle. BW normalized lumbar compressive loads were correlated with T12-S1 balance and sacral angle. BW normalized lumbar disc shear (compressive) loads increased (decreased) significantly with decreasing lumbar lordosis. Cervical compressive stresses and loads were correlated with all sagittal balance parameters except S1-HA and T12-S1. A neutral spine sagittal model was constructed from the 67 subjects.

CONCLUSIONS: The analyses suggest that sagittal spine balance and curvature are important parameters for postural load balance in healthy male and female subjects. Morphological predictors of altered disc load outcomes were sagittal balance parameters in the thoracic spine and anatomic angles in the lumbar spine. © 2005 Elsevier Inc. All rights reserved.

Keywords: Biomechanical modeling; Posture; Kyphosis; Spine; X-ray; Morphology

Introduction

Alterations in spinal balance and curvature are deemed by many investigators to be implicated in the development of a variety of spinal disorders, including acute and chronic low back pain [1,2], disc degeneration [3–6], spondylosis [3,7], ossification of spinal ligaments [8,9], adolescent idiopathic scoliosis [10,11], Scheuermann's kyphosis [12], impaired ribcage expansion [13,14], early osteoarthritis and disc degeneration [14,15], osteoporosis and vertebral compression fractures [14,16], and spondylolisthesis [17]. Before surgical or conservative rehabilitative treatment is initiated, factors affecting the balance and curvature of the spine must be identified and understood. This implies a need to define a normal or "ideal" spinal morphology (balance and curvature). Hence, a number of studies have focused on documenting the sagittal morphology of the spine [18–26].

Interactions between low back pain and spine morphology have been reported [27–31]. In a group of 124 normal and low back pain subjects, Harrison and associates [1] found that several lumbar morphological measurements, including segmental and total lumbar lordosis, were capable of discriminating normal subjects from acute low back pain sufferers (hyperlordotic) and chronic low back pain sufferers (hypolordotic). Harrison and associates hypothesized that the origin of pain in the chronic group was abnormal disc loads associated with loss of lordosis. Lumbar lordosis has also been suggested to be an anatomic [32] and mechanical necessity for upright posture and locomotion [33,34]. The degree of abnormal kyphotic thoracic curvatures has also been associated with a variety of clinical syndromes. Noteworthy, increased thoracic kyphosis occurs with advanced aging and is an indicator of thoracic vertebral compression fractures leading to pain [12,13,15,16,35].

Although sagittal profiles of the thoracolumbar spine have been hypothesized to influence spinal coupling [6,36,37] and loads on spinal tissues [5,7,38], this has not been documented in a systematic manner. The aims of the current study were to 1) measure variations in spinal morphology on standing lateral radiographs of asymptomatic subjects, and 2) investigate the interaction between spinal column morphology and intervertebral disc loads and stresses.

Methods

Sixty-seven human subjects (chiropractic students) participated in this study. Subjects were young (mean age=26.7, SD 4.8 years, n=67) and asymptomatic (mean Numerical Rating Scale [NRS]=1.1, SD 1.1) at the time of the examination. The subjects had no prior history of back pain requiring medical attention. The average body weight (BW) and height of the subjects was 78.8 kg (SD 16.3, range 50 to 118) and 176 cm (SD 9.6, range 146 to 191), respectively. There were 51 male subjects (mean age=26.6, SD 5.2 years) and 17 female subjects (mean age=27.1, SD 3.4 years). In addition to providing basic demographic data, subjects reviewed the Institutional Review Board approved study protocol and provided informed consent for their participation.

Segmental and global measurements of spine sagittal curvature and balance were obtained from digitized lateral full-spine X-rays of neutral posture, upright standing human subjects. X-Y coordinates of the anterior-superior, posterior-superior, anterior-inferior, and posterior-inferior corners of each vertebral body (VB) from C2-S1 were marked using a sonic digitizer (GP-9; GTCO CalComp, Columbia, MD). The resolution of the sonic digitizer was 0.125 mm. Additional details of the radiographic measurement procedure are found elsewhere [39,40].

A sagittal plane, upright posture, quadrilateral element geometric model of the anterior spinal column (C2-S1) of each subject was created using the digitized VB coordinate data. From the models, several segmental and global morphological measurements of anatomic angles were obtained using a previously reported posterior tangent technique [39–41]. The posterior tangent method of Harrison uses the posterior-superior and posterior-inferior corners of each VB to form tangent lines. The posterior margins of the VBs are less subject to degenerative (osteoarthritic) changes in comparison to the anterior margins or end plates, which makes anatomic angle measurements more reliable and valid in comparison to other methods [39–41]. In this study, absolute rotation angles (ARA) between T1-T12 (thoracic kyphosis angle) and T12-S1 (lumbar lordosis angle) were computed (Fig. 1). The pelvic angle, defined as the angle between the hip axis and the posterior inferior body corner of S1, Ferguson's angle (FA), defined as the angle between horizontal and a line through the superior S1 end plate, and

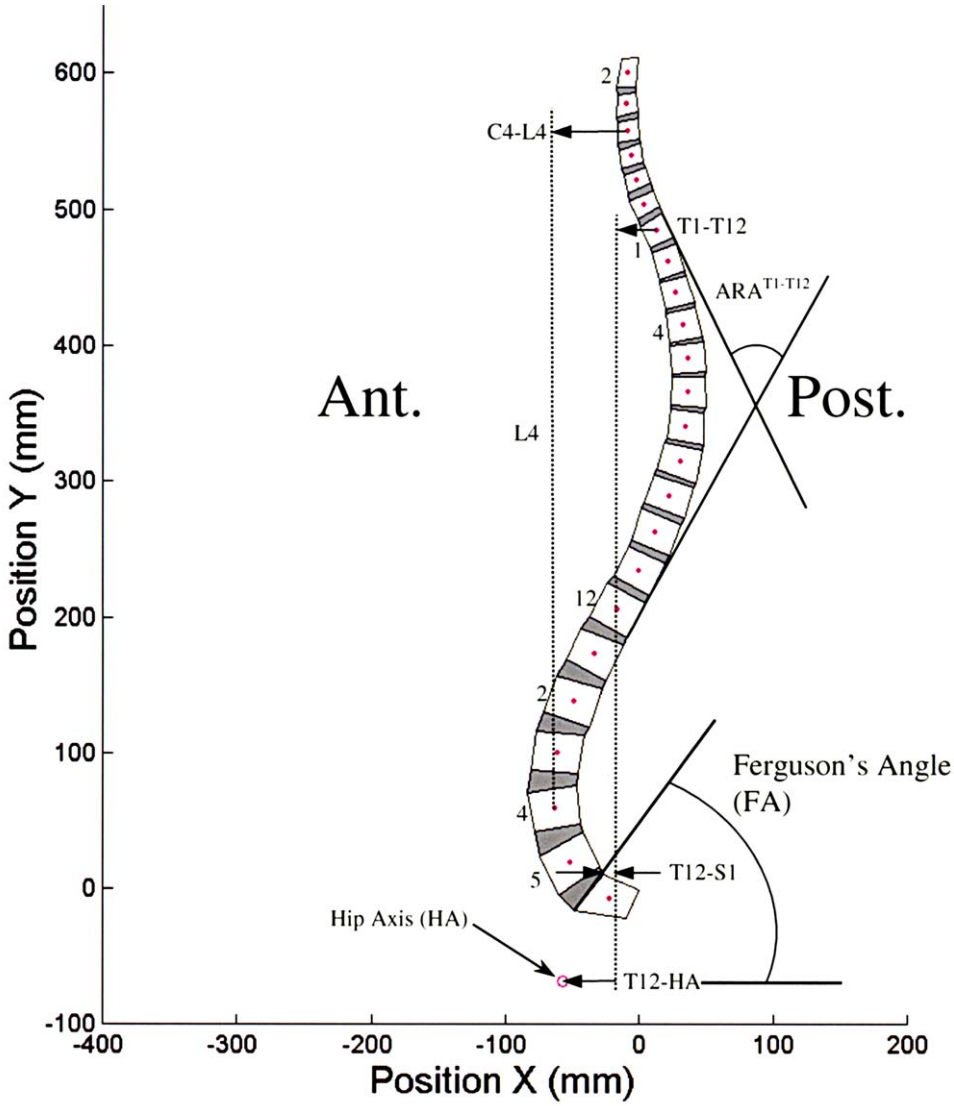

Fig. 1. Quadrilateral element model (Subject 20) and posterior tangent spine curvature measurement technique after Harrison et al. [41]. Relative rotation angles were measured using a tangent line along the posterior margin of vertebral body for each vertebral segment and for the thoracic spine area (ARA^{T1-T12}). Several sagittal balance parameters were measured, including C4-L4, C7-S1 (not shown), T1-T12, T4-S1 (not shown), T12-S1, HA-T4 (not shown), HA-T12, HA-S1 (not shown).

several sagittal balance parameters (posterior-anterior distance between VB centroids) were also computed. Definitions of each of the morphological parameters examined in this study are summarized in Table 1. Spinal column height, defined as the difference between the most superior C2 VB Y-coordinate and the most inferior S1 Y-coordinate, was also calculated.

All anatomic angle and sagittal balance measurements were performed using Matlab (The MathWorks, Natick, MA). Intervertebral disc (IVD) and VB centroids were computed from the quadrilateral element X,Y-coordinates using an areal analysis algorithm [42]. IVD and VB centroids were used to construct a composite sagittal profile model of the C2-S1 spine.

A postural loading model [16,43] was used to determine postural loads and stresses acting on the C2-S1 intervertebral discs. For this analysis, the quadrilateral element model geometry of each subject was used as the input to the model, which computed postural shear and compressive loads and stresses for each IVD segment. A local coordinate system was defined for each segment with the shear and compression axes oriented parallel and perpendicular, respectively, to the line bisecting each IVD. Loads were determined at the anterior and posterior margins of the IVD (along disc bisector) and at the IVD centroid. Postural loads were based upon the BW load above each vertebral segment with the line of gravity (LOG) initially positioned 10 mm anterior to the centroid of the L4 VB (refer to Fig. 1). The location of the LOG, BW load above each segment, values for the posterior muscle moment arms, and disc cross-sectional areas for the C2-S1 segments were based upon previously published data for a 70-kg, 174-cm subject [43,44], but

Table 1
Descriptions of the standing lateral radiograph sagittal balance (alignment) and sagittal curvature (angle) parameters

Parameter	Abbreviation	Description
Sagittal alignment, C4-L4	C4-L4	Perpendicular distance between C4 (centroid) and L4 (centroid) plumblines (mm)
Sagittal alignment, T1-T12	T1-T12	Perpendicular distance between T1 (centroid) and T12 (centroid) plumblines (mm)
Sagittal alignment, T12-S1	T12-S1	Perpendicular distance between T12 (centroid) and S1 (posterior-superior VB corner) plumblines (mm)
Sagittal alignment, C7-HA	C7-HA	Perpendicular distance between C7 (centroid) and HA plumblines (mm)
Sagittal alignment, T4-HA	T4-HA	Perpendicular distance between T4 (centroid) and HA plumblines (mm)
Sagittal alignment, S1-HA	S1-HA	Perpendicular distance between S1 (posterior-superior VB corner) and hip axis (HA) plumblines (mm)
Sagittal alignment, C7-S1	C7-S1	Perpendicular distance between C7 (centroid) and S1 (posterior-superior VB corner) plumblines (mm)
Sagittal alignment, T4-S1	T4-S1	Perpendicular distance between T4 (centroid) and S1 (posterior-superior VB corner) plumblines (mm)
Thoracic kyphosis angle	ARA^{T1-T12}	Absolute rotation angle formed by posterior vertebral body tangent lines of T1 and T12 (degrees)
Lumbar lordosis angle	ARA^{T12-S1}	Absolute rotation angle formed by posterior vertebral body tangent lines of T12 and S1 (degrees)
Lumbo-sacral angle	ARA^{L4-S1}	Absolute rotation angle formed by posterior vertebral body tangent lines of L4 and S1 (degrees)
Ferguson's sacral base angle	FA	Angular measurement between horizontal and a line through the superior S1 end plate (degrees)
Pelvic tilt angle	PA	Angular measurement between horizontal and a line from the superior acetabulum of the posterior-inferior vertebral body of S1 (degrees)

ARA=absolute rotation angles; FA=Ferguson's angle; HA=hip axis; PA=pelvic angle; VB=vertebral body.

scaled to the weight and height of the subjects in this study. Only the anterior column of the spine was considered, and ligamentous structures were not explicitly modeled. In this static upright posture model, equilibrium is based solely upon the balance of BW forces and posterior trunk muscles forces (erector spinae muscle). Although the effects of trunk muscle synergism (contribution of anterior muscles), passive spinal tissues (ligament load sharing), and intra-abdominal pressure are not considered, the model force predictions show good agreement with other experimental and analytical studies [16,43].

Average values of the IVD loads (shear and compression loads normalized with respect to BW) and IVD stresses (shear and compression) were computed for the following regions: whole spine (C2-S1), cervical (C2-T1), thoracic (T1-L1), and lumbosacral (L1-S1), resulting in a total of 16 IVD biomechanical parameters. A least-square, linear regression analysis was used to examine correlations between the morphologic parameters (sagittal balance, anatomic angles) and the three regional and whole spine biomechanical parameters (BW normalized loads, stresses).

Statistical analyses

Frequency distributions (histograms) and distribution characteristics (skew, kurtosis) were performed on the morphological data. Morphological anatomic angle parameters were also used to subdivide the subjects according to the following criteria: Ferguson's sacral base angle (FA), lumbosacral angle (ARA^{L4-S1}), and thoracic kyphosis (ARA^{T1-T12}), each normalized with respect to the lumbar lordosis angle (ARA^{T12-S1}). For each of these criteria, the subjects were partitioned into four groups constructed from the quartiles of the measurements. The mean regional biomechanical parameters for each quartile were then compared using a one-way analysis of variance (ANOVA). The normality and homogeneity of variance assumptions were met for all 48 analyses (3 morphological criteria×16 biomechanical parameters). Statistically significant ANOVAs were followed by Tukey's multiple comparison procedure to discern the nature of pairwise differences. Because a large number of ANOVAs were performed, in order to protect against errors of incorrectly finding differences when none exist, significant differences identified by the ANOVA were only followed up by the Tukey procedure when the ANOVA p value was less than .0001.

Results

In this group of normal male and female subjects, the average ratio of spinal column height (C2-S1) and body height was 0.35 (range 0.30 to 0.42), indicating that in the neutral, upright posture the spine was approximately one-third of the body height. Considerable variation in neutral, upright posture sagittal balance and anatomic angles was observed among the subjects (Table 2). Posterior-anterior variations in sagittal balance (minimum to maximum) spanned a range from 59.5 mm (S1-HA) to 96.7 mm (T4-S1). Frequency distributions for selected balance parameters (C4-L4, T1-T12, and T12-S1) are shown in Figure 2. C4-L4 balance showed a flattened (negative kurtosis), relatively symmetric (low skew) frequency distribution, whereas the T1-T12 balance was more peaked (low kurtosis) and more skewed. T12-S1 balance was the most symmetric. C7-S1, T1-T12, and T12-S1 sagittal balance parameters showed the lowest average posterior-anterior misalignment (−5.3 mm, −0.04 mm, and +12.1 mm, respectively), but each exhibited a range of over 80 mm (Table 2). The hip axis (HA) sagittal balance parameters (C7-HA, T4-HA, S1-HA) showed the least overall variance (SD/mean). Of the anatomic angle measures, thoracic curvature (ARA^{T1-T12}) and lumbo-sacral angle (ARA^{L4-S1}) showed the highest symmetry, whereas pelvic angle and FA exhibited the least symmetric frequency distributions (Table 2 and Fig. 3). Thoracic kyphosis angle (ARA^{T1-T12}) showed the least overall variance among the subjects (Table 2).

Table 2
Summary of sagittal balance and anatomic angles obtained from analysis of neutral, upright standing posture radiographs. Minimum, maximum, skew, kurtosis, and mean (standard deviation) for 67 subjects

Parameter*	Minimum	Maximum	Skew†	Kurtosis†	Mean (SD)
C4-L4 (mm)	−24.4	72.1	−0.11	−0.89	23.7 (23.4)
T1-T12 (mm)	−57.8	−27.6	−0.46	−0.01	−0.04 (20.6)
T12-S1 (mm)	−27.6	55.8	−0.03	0.29	12.1 (15.6)
C7-HA (mm)	13.5	77.9	−0.31	−0.37	35.2 (22.6)
T4-HA (mm)	16.2	115.0	−0.21	0.07	64.1 (21.1)
S1-HA (mm)	−4.4	55.1	−0.54	0.41	29.8 (11.9)
C7-S1 (mm)	−42.8	46.3	−0.39	−0.67	5.3 (23.2)
T4-S1 (mm)	−15.0	81.7	−0.43	0.25	34.3 (19.5)
ARA^{T1-T12} (degrees)	16.3	71.5	−0.06	−0.15	43.7 (11.4)
ARA^{T12-S1} (degrees)	−97.4	−41.1	−0.31	−0.06	−67.4 (12.6)
ARA^{LA-S1} (degrees)	−69.9	−24.0	0.20	0.39	−48.1 (9.8)
FA (degrees)	32.4	58.8	0.40	−0.24	44.1 (5.7)
PA (degrees)	33.7	83.7	0.97	1.31	49.4 (9.9)

* See Table 1 and Figure 1 for abbreviations and descriptions of measurements using Harrison posterior tangent (angles) and plumbline techniques (horizontal translation, mm). Sagittal balance parameters C4-L4, T1-T12, T12-S1, C7-HA, T4-HA, S1-HA, C7-S1, and T4-S1 are the perpendicular distances from the respective quadrilateral element VB centroids.

† Skewness and kurtosis indicate distribution asymmetry and flatness, respectively.

The postural loading model indicated that anterior and posterior IVD loads were balanced at T8-T9 and showed the greatest difference at L5-S1 (Fig. 4). The pattern of IVD postural stresses (compression, shear) mirrored the sagittal curvatures of the spine and showed less overall variation (2.3 fold, 1.8 fold) than the corresponding postural loads. The average compressive postural loads acting on the IVD centroid ranged from 13.8% of BW (C2-C3) to 94.3% BW

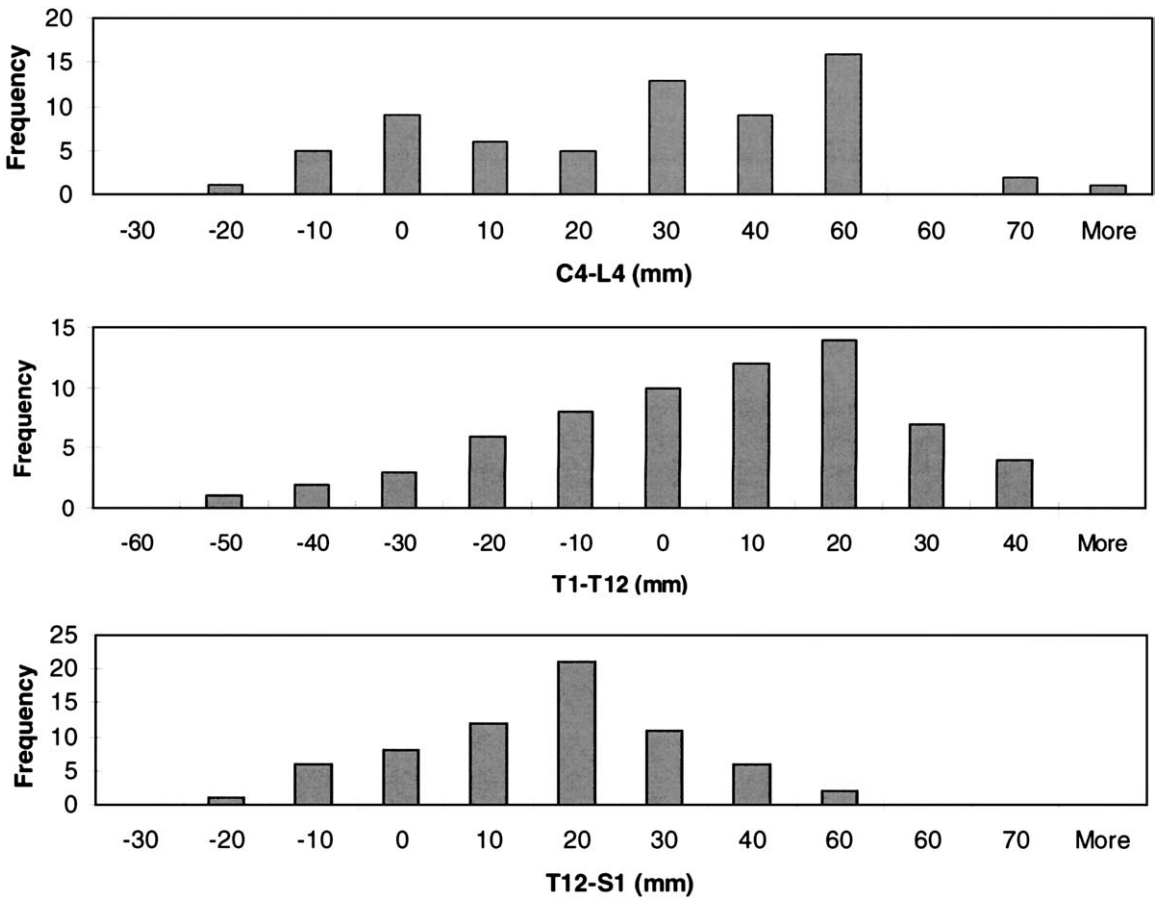

Fig. 2. Morphological analysis results for neutral posture sagittal balance. Histograms for C4-L4, T1-T12, and T12-S1 sagittal alignment are illustrated. Each bar represents the number of data points between the current bin number and the adjoining higher bin.

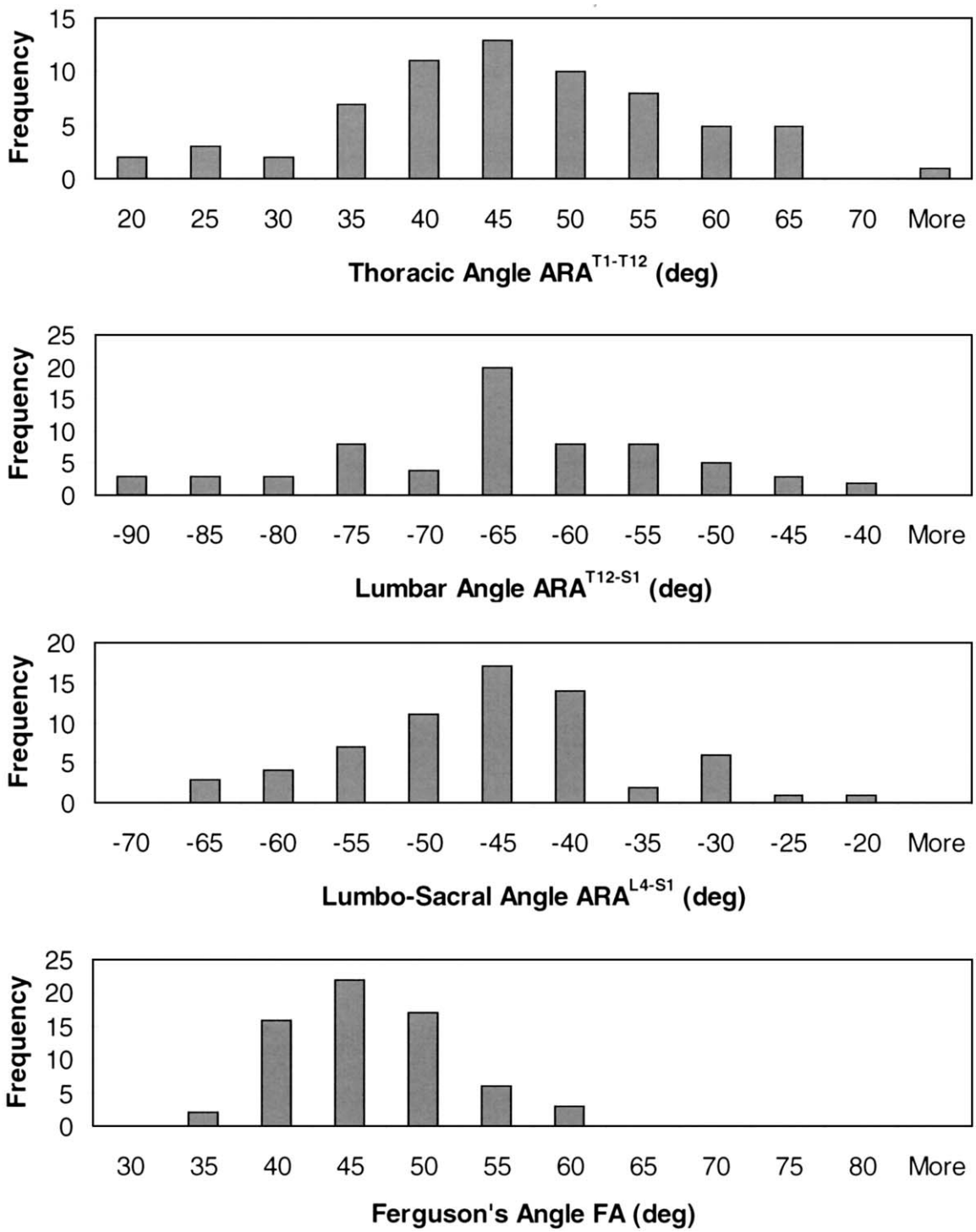

Fig. 3. Morphological analysis results for neutral posture sagittal profile. Histograms for ARA^{T1-T12}, ARA^{T12-S1}, ARA^{L4-S1}, and Ferguson's angle (FA) curvatures are illustrated. Each bar represents the number of data points between the current bin number and the adjoining higher bin.

(T11-T12). Mean IVD compressive loads (% BW) for the cervical (C2-T1), thoracic (T1-L1), and lumbar (L1-S1) regions were 15.2% (SD 5.0), 61.9% (SD 6.8), and 65.1% (SD 2.0), respectively. Compressive stresses were highest in the mid-thoracic region of the spine, whereas shear stresses were lowest at T6-T7 and highest at L5-S1 (Fig. 5).

Significant ($p<.001$) linear correlations ($r>.37$) were found between a number of postural load parameters and sagittal morphology variables (Table 3). Thoracic shear stresses were correlated with sagittal balance variables (C7-HA, T4-HA, C7-S1, T4-S1, C4-L4, T1-T12), but were poorly correlated to sagittal anatomic angles. Lumbar shear

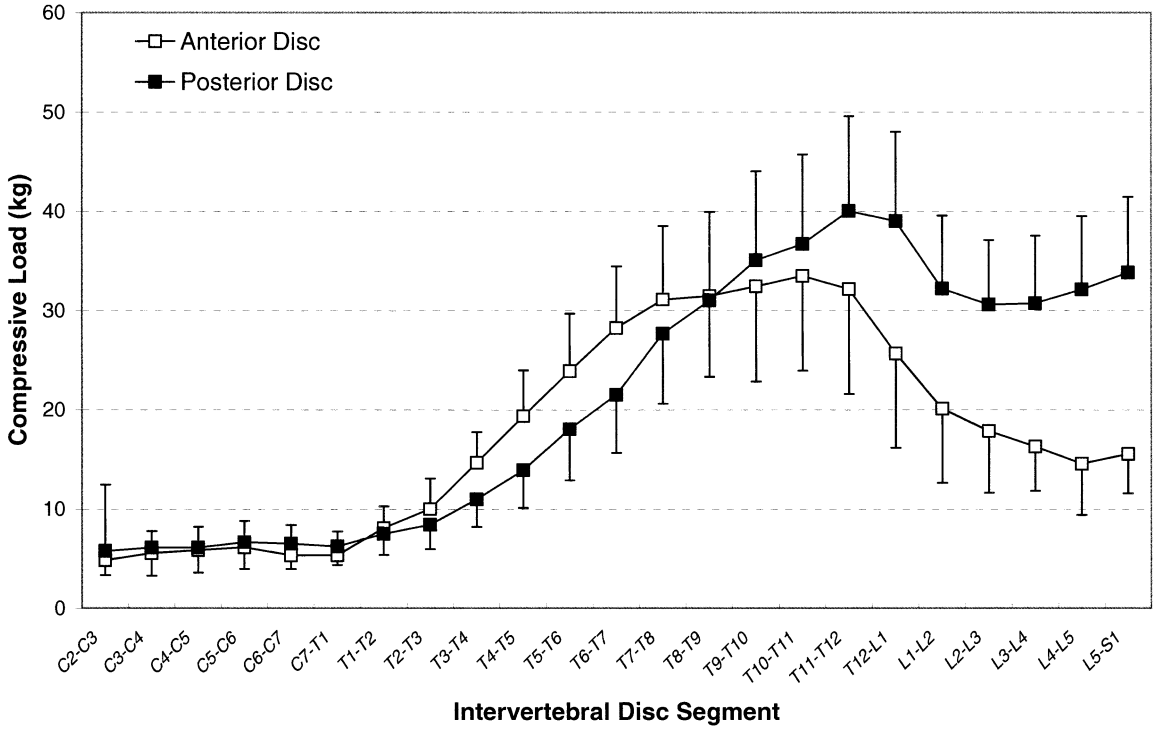

Fig. 4. Distribution of anterior and posterior intervertebral disc compressive loads along the C2-S1 spine. Symbols and error bars represent mean and standard deviation, respectively, of the 67 subjects.

stresses were closely correlated with T12-S1 sagittal balance and showed a significant correlation with lumbar angle (ARA^{T12-S1}) and sacral angle (FA). Cervical and thoracic compressive stresses were correlated with several sagittal balance variables, most notably C7-HA, T4-HA, and C7-S1, but not to anatomic angles. BW normalized thoracic shear loads were well correlated to the sagittal balance variables. BW normalized compressive loads were closely correlated with sagittal balance parameters in both the cervical and thoracic regions. FA was positively correlated with lumbar shear loads (% BW) and lumbar compressive loads (% BW). In general, intervertebral disc stresses and loads were greatest in subjects with sagittal posture imbalance. Anterior translation of cervical and thoracic segments relative to the hip axis was associated with increased IVD postural stresses and loads.

The quartile analysis revealed only a few significant differences within the mean regional biomechanical parameters for each quartile, and these differences were limited to quartiles of the anatomic angle ratio ARA^{L4-S1}/ARA^{T12-S1} (Q1=0.44 to 0.62; Q2=0.62 to 0.71; Q3=0.71 to 0.82; Q4=0.82 to 1.06). Noteworthy was the finding that lumbar shear loads (normalized to BW) decreased significantly with increasing ARA^{L4-S1}/ARA^{T12-S1} ratio (Q1 and Q2>Q4, Q1>Q3, $p<.0001$). Conversely, lumbar compressive loads (normalized to BW) increased significantly with increasing ARA^{L4-S1}/ARA^{T12-S1} ratio (Q3 and Q4>Q1, $p<.0001$). These findings are graphically summarized in Figure 6.

An average neutral posture spine model was constructed from the 67 subjects (Fig. 7). Plumblines drawn from C7 and T1 clearly illustrate the upright posture sagittal balance of C7-S1 and T1-T12. In the composite model, the L3 VB centroid was located 6.4 mm anterior (along posteroanterior x-axis) to the femoral head centroid (X, Y-coordinate= −48.7, −62.7 mm). X, Y coordinates corresponding to the C2-S1 composite model VB (and IVD) quadrilateral element centroids are summarized in Table 4.

Discussion

Sagittal curvatures (lumbar lordosis, thoracic kyphosis) and pelvic rotation are geometric parameters that are known to have a significant influence on mechanical properties during compressive loading [37,45–51]. Hence, a well-defined, normal thoracolumbar spine sagittal morphology is important for understanding spine biomechanics. In this study, a postural loading model [16,43] was used to systematically investigate the relationship between sagittal morphology and postural loads and stresses acting on the intervertebral discs.

One of the aims of the current study was to detail the variation in spinal column morphology on standing lateral radiographs of asymptomatic male and female subjects. A number of studies have performed similar segmental analyses of sagittal plane alignment and balance using lateral

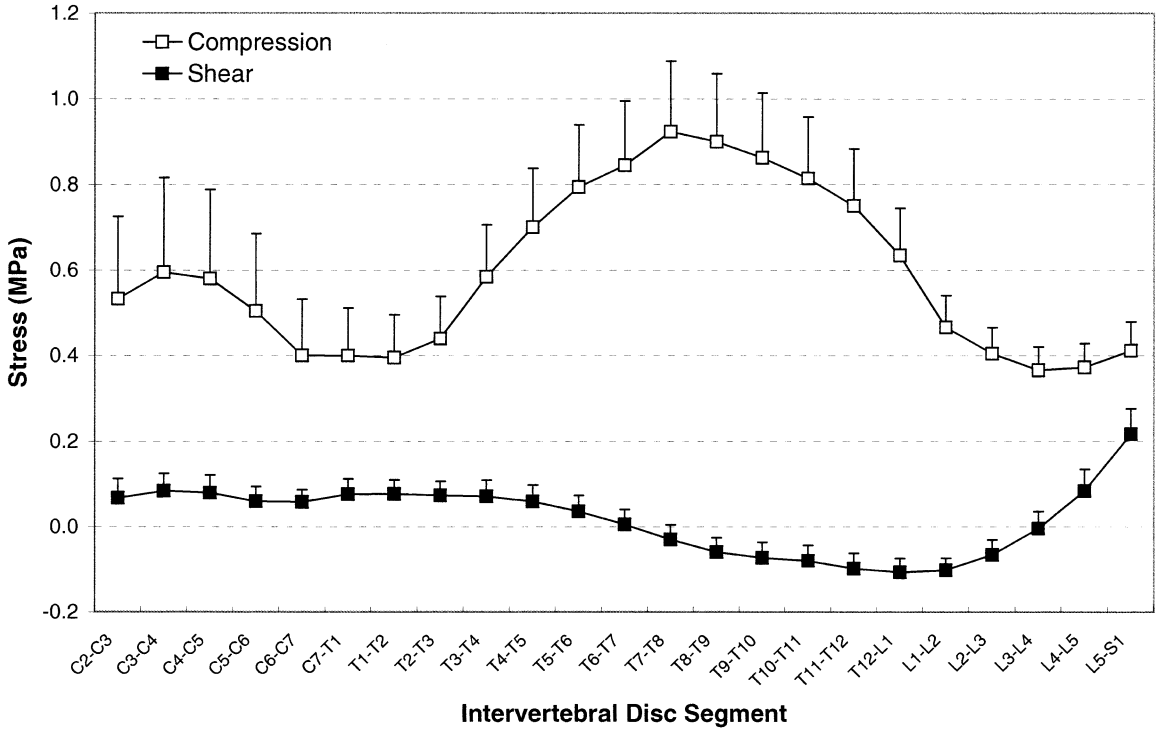

Fig. 5. Distribution of intervertebral compressive and shear postural stresses along the C2-S1 spine (IVD centroids). Symbols and error bars represent mean and standard deviation, respectively, of the 67 subjects.

standing radiographs of the lumbar spine [24,52,53] and thoracolumbar spine [20,21,25,29,54–56] of asymptomatic subjects. Examination of the literature indicates that there is large variability in sagittal balance and alignment parameters in asymptomatic subjects, which do not appear to be race-related [52,54] or gender-related [20,21,24,25,29]. However, weak age-related alterations in sagittal alignment have been reported where adolescents tend to stand with greater posterior sagittal balance [20] and seniors have forward sagittal balance with increased thoracic kyphosis [57]. Our study focuses on a group of similar age asymptomatic male and female subjects and, like previous investigations, considerable variation in neutral, upright posture sagittal balance and anatomic angles was observed. In addition, interactions between spinal morphology and intervertebral disc loads and stresses were observed. Discussion of these interactions follows.

To begin, our biomechanical and morphological analyses indicated that lumbar shear loads increased with decreasing lumbar lordosis (decreasing $ARA^{L4\text{-}S1}/ARA^{T12\text{-}S1}$ ratio).

Table 3
Correlation (correlation coefficients) of sagittal balance parameters, anatomic angles, and regional intervertebral disc postural loads (% BW) and stresses

Parameter	C7-HA	T4-HA	S1-HA	C7-S1	T4-S1	C4-L4	T1-T12	T12-S1	$ARA^{T12\text{-}S1}$
Shear stress (C2-S1)	−.643	−.461	.371	−.817	−.724	−.815	−.622	−.341	.103
Lumbar	−.233	−.296	.183	−.321	−.432	−.055	.299	−.890	−.437
Thoracic	−.732	−.522	.120	−.775	−.637	−.844	−.951	.147	.274
Cervical	.039	.147	.389	−.161	−.077	−.303	−.092	−.060	.207
Compressive stress (C2-S1)	.565	.544	.015	.544	.580	.531	.433	.249	−.212
Lumbar	−.035	.052	.177	−.124	−.051	−.163	−.143	.045	−.058
Thoracic	.434	.529	.119	.363	.500	.310	.212	.306	−.194
Cervical	.751	.539	.187	.828	.698	.885	.783	.147	−.250
Shear load (C2-S1)	−.715	−.691	.223	−.811	−.883	−.631	−.364	−.728	−.090
Lumbar	−.203	−.283	.148	−.274	−.397	.008	.345	−.890	−.487
Thoracic	−.733	−.628	.043	−.737	−.706	−.801	−.891	.096	.426
Cervical	.090	.209	.370	−.102	.001	−.282	−.089	.030	.225
Compressive load (C2-S1)	.748	.737	−.194	.829	.916	.756	.450	.643	−.263
Lumbar	.161	.187	−.307	.314	.390	.134	−.227	.775	.267
Thoracic	.679	.750	−.122	.724	.886	.627	.314	.691	−.282
Cervical	.812	.569	−.270	.929	.779	.988	.851	.190	−.276

ARA=absolute rotation angles; BW=body weight; HA=hip axis.
Correlations greater than .37 or less than −.37 were significant at $p<.001$ or more.

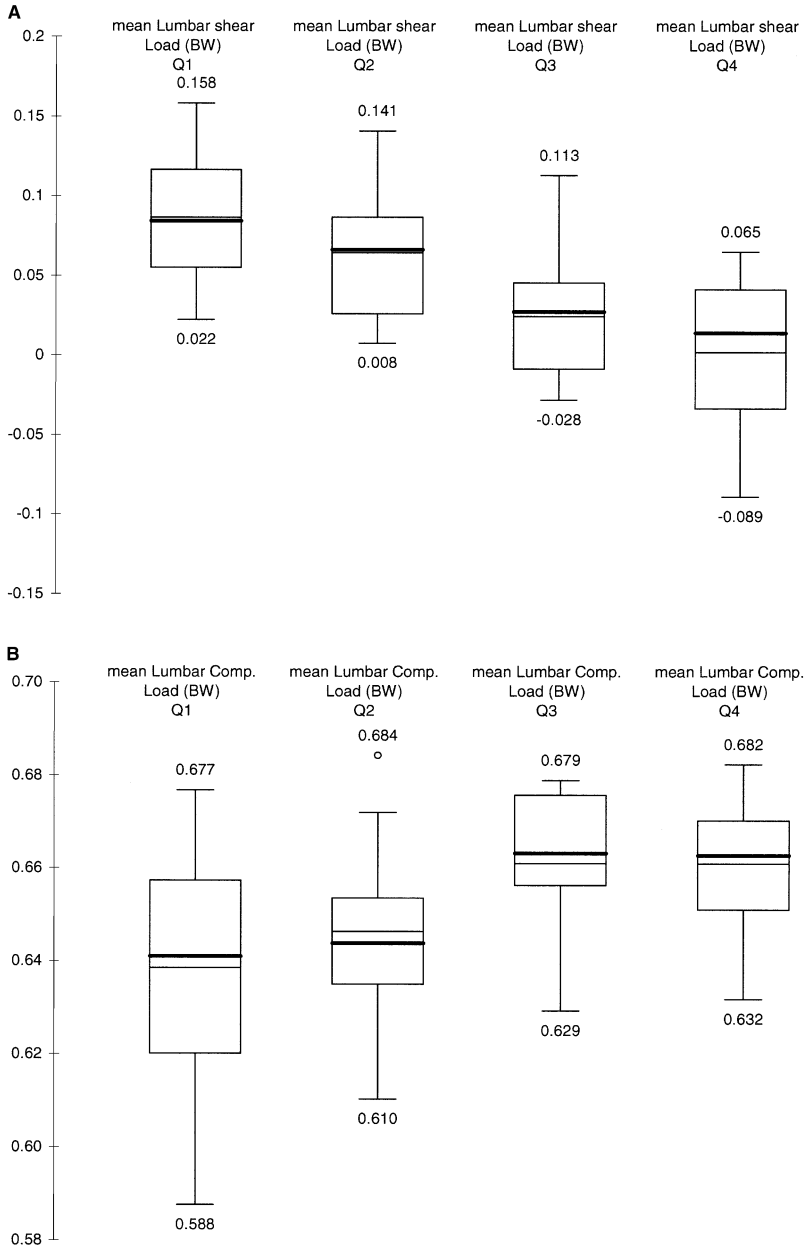

Fig. 6. Box plot summary of the quartile analysis for the ratio $ARA^{L4\text{-}S1}/ARA^{T12\text{-}S1}$. Increasing $ARA^{L4\text{-}S1}/ARA^{T12\text{-}S1}$ ratio corresponds to increasing lumbar lordosis. (A) The first quartile (Q1) and second quartile (Q2) have significantly greater ($p<.0001$) mean lumbar shear load (BW) responses than the fourth quartile (Q4). Q1 has a significantly greater ($p<.0001$) mean lumbar shear load (BW) response than the third quartile (Q3). (B) Q1 has a significantly lower ($p<.0001$) mean lumbar compressive load (BW) response than Q3 or Q4.

Using cadaveric lumbar spines tested in axial load, Umehara et al. [5] also found increased posterior shear stresses as a consequence of an 8° reduction of the L4-S1 lordosis. The change in loading from compression to shear, with loss of the distal lordosis, may have clinical relevance to low back pain and disc degeneration. For example, in asymptomatic normal subjects, the distal lumbar lordosis (L4-S1) comprises approximately 65% of total lordosis [20,21,24,29,54] and, mechanically, the normal lumbar spine is best suited to withstand compressive loads [23,58]. In comparison to normal subjects, chronic low back patients with and without lower lumbar degenerative discs have been found to have a statistically significant reduction in the distal lumbar lordosis [1,29,31,55]. In subjects with reduced distal lumbar lordosis, the increased shear loads may well trigger an increase in matrix metalloproteinases leading to sensitization of nociceptive neurons and eventual degradation of disc tissue [59,60].

Second, of clinical importance was the finding that lumbar shear stresses were closely correlated with T12-S1 sagittal balance, with lumbar lordosis, and with sacral angle (FA). Jackson and associates [55] found that hyperlordosis of the lumbar spine was present in 30 patients with Grades I and II L5-S1 spondylolisthesis. Hypothesizing that increased shear

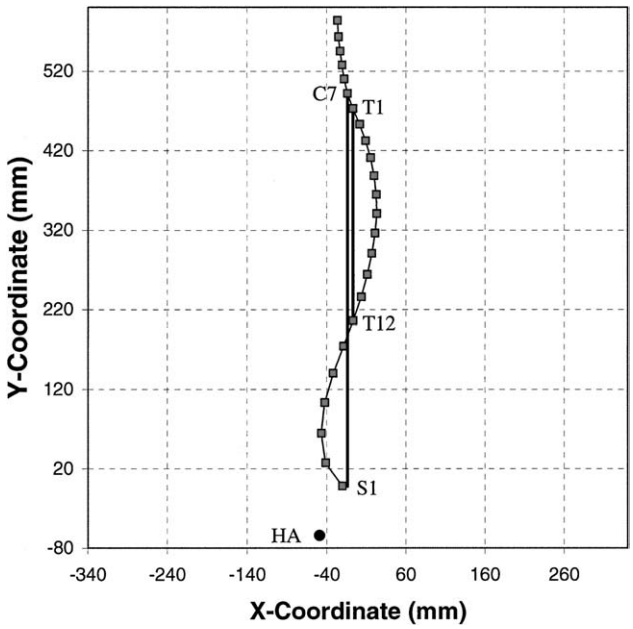

Fig. 7. Neutral spine ensemble average sagittal profile model (vertebral body centroids) derived from the quadrilateral element models of all 67 subjects examined in this study. Sagittal balance parameters, T1-T12 and C7-S1, are shown illustrating the vertical alignment of these segments in the upright posture.

Table 4
X-Y coordinates of the neutral posture ensemble average model. Vertebral body (VB) and intervertebral disc (IVD) centroid coordinates defined relative to the posterior-inferior corner of the S1 VB (digitizing tablet X,Y-coordinate origin)

	VB Centroid		IVD Centroid	
Segment	X-coor. (mm)	Y-coor. (mm)	X-coor. (mm)	Y-coor. (mm)
C2	−26.34	583.58		
C3	−25.18	562.96	−26.36	575.25
C4	−23.05	544.86	−24.34	553.73
C5	−20.52	527.39	−21.94	536.03
C6	−17.83	509.94	−19.46	518.67
C7	−13.59	491.80	−16.51	501.01
T1	−6.81	472.76	−11.03	482.65
T2	1.49	452.90	−2.78	463.16
T3	9.16	432.31	5.77	443.06
T4	15.36	410.84	12.94	422.11
T5	20.00	388.11	18.60	399.86
T6	22.70	364.75	22.18	376.63
T7	23.29	340.54	23.88	352.79
T8	21.13	315.73	22.81	328.24
T9	16.90	290.37	19.14	303.29
T10	11.10	263.92	13.95	277.57
T11	3.48	235.71	7.26	250.24
T12	−6.77	205.81	−2.11	221.32
L1	−18.83	174.14	−14.09	190.80
L2	−31.86	139.94	−27.09	157.90
L3	−42.37	103.01	−39.59	122.06
L4	−46.73	64.66	−47.58	83.76
L5	−41.20	27.12	−47.89	44.96
S1	−20.14	−2.13	−35.53	8.31

stresses were the cause of spondylolisthesis, Rajnics and colleagues [61] found increased lumbar lordosis and sacral angle in patients with spondylolisthesis matched to normal controls. Using a sagittal balance measurement from L1 centroid to posterior superior of S1, Kawakami et al. [62] identified an anterior displacement of greater than 35 mm to adversely affect the recovery in 47 surgically treated patients with degenerative spondylolisthesis. In fact, anterior to posterior thoracic translations can cause a net change in thoracic kyphosis of 26° and 31° in sacral angle [63]. Thus, the increased shear stresses resulting from a forward displaced sagittal balance, increased sacral angle, and lumbar angle could be a likely mechanism for the development, progression, or exacerbation of spondylolisthesis.

Third, the model prediction of increased IVD postural stresses and loads associated with anterior translation of cervical and thoracic segments relative to the hip axis may have implications for conditions such as upper and low back pain [63], post-fusion adjacent segment disc degeneration [4], osteoporotic deformity [16], and age-related increases in anterior sagittal postural balance [57]. In general, our model predictions indicated that intervertebral disc stresses and loads were greatest in subjects with sagittal posture imbalance. This result agrees qualitatively with previously published studies on sagittal postural displacements in the cervical [64] and thoracolumbar regions [38].

The predicted sagittal spine/posture induced load changes may expose the IVD to an abnormal stress environment. Apparently, the IVD is well suited for this situation because the IVD stresses showed less overall variation (2.3 fold, 1.8 fold) than the corresponding postural loads. Nonetheless, because the pattern of IVD postural stresses mirrored the sagittal curvatures and sagittal displacement of the spine, a failure of the IVD's hydrostatic mechanism under these sustained loads could occur. In the sagittal plane, progression of kyphotic deformities follows mechanical loading (Hueter-Volkmann law) where increased compression loads are known to cause deformity accentuation [12]. However, increased dorsal kyphosis as a result of aging has been shown to be closely related to the integrity of the IVD as well [65]. Our findings, of increased thoracic IVD compression load with increased thoracic kyphosis and increased IVD compression and shear loads with increased sagittal balance displacement, might prove to be a logical mechanism for IVD deformity causation and progression in the thoracic region.

The spine morphological data and quadrilateral element data presented in this study should be useful for future analytical and numerical studies of the normal and pathological spines. One of the areas of interest should be that of compensated/uncompensated spinal balance in terms of sagittal alignment parameters. In general, as the thoracic kyphosis increases the lumbar lordosis is also seen to increase [55]. As an example, in Scheuermann's kyphosis, hyperlordosis of the lumbar spine is known to occur with

the cervical spine adopting a curvature that is the net difference between the two lower curves (compensated) [66]. However, in patients with spondylolisthesis, total kyphosis is shown to decrease with increased lumbar lordosis. An analysis of postural load and IVD stresses assists in understanding why different deformities are compensated (or uncompensated) and may help to explain when postural geometry/load imbalance is associated with increased risk of deformity.

Investigators have reported interactions between low back pain and biomechanical changes of the lumbar spine, including changes in lumbar curvature [1,29,31,55,67] and intervertebral disc height [28]. Clinical evaluation of spine morphology and postural load balance in acute and chronic back pain patients is therefore needed for at least two primary reasons: 1) to isolate morphological parameters that might provide clinicians with diagnostic tools to decide when an individual might be at risk of a first time experience of pain requiring treatment intervention, and 2) to identify areas of likely deformity progression/development in an individual spine. The postural disc load and spinal morphology interactions identified in this study have clinical implications for the ideal sagittal spine geometry.

When developing a biomechanical model, it is often necessary to make a number of assumptions in order to avoid as much excess complexity as is practical within the constraints of validity. The quadrilateral element model used in this study, and applied to the neutral, standing posture, is a single muscle model designed to provide an overview of the loading profile of a complex mechanical system. This static model has been used in previous studies to examine IVD and VB loads and stresses in conjunction with body height changes [43], thoracic deformity [16], and anterior translated postures [68]. These studies provide additional details and validation of the model, and indicate that the magnitude of predicted cervical, thoracic, and lumbar loads and stresses is consistent with previous experimental studies. Several model-specific assumptions, however, warrant additional elaboration. Firstly, the X-ray-based quadrilateral element model does not incorporate the load sharing characteristics of the passive spinal tissues, although it is known that these tissues do contribute to the restorative moment of the spine [69,70]. Secondly, stresses were computed using a local coordinate system oriented with respect to the IVD bisector. Thirdly, and perhaps most noteworthy, is our assumption that the location of the center of mass (COM) is constant, acting along a fixed LOG or "line of gravity". According to a computed tomography study conducted by Pearsall et al. [71], the COM shows a curvilinear change from T4 to L5 with an average deviation of the COM relative to L4 of 5.9 mm. Small deviations in the COM have a very small overall effect on the LOG-based shear and compressive force predictions for segments L5 and above, but are more problematic for force estimates at L5-S1 where the deviation of the COM from a fixed LOG is marked (about 20 mm). Previous biomechanical studies indicate that the upright posture L5-S1 anterior-posterior shear is generally less than or equal to one-fifth of compressive force [72,73], which is substantially lower than the ratio obtained in this study (mean L5-S1 shear/compression ratio=0.53). However, because the main outcome measures reported in the current study were based on a region-by-region analysis of IVD loads, the overall influence of COM variations on the biomechanical results and conclusions is minor.

Conclusions

In this study we have presented a mathematical analysis of postural disc loads and sagittal balance parameters based on digitized radiographs of asymptomatic subjects. Postural load analyses and identification of spinal geometry can be used for clinical comparisons, and may be used to discriminate between normal subjects and those with low back pain. The sagittal plane quadrilateral element geometric model data will also assist researchers in developing mathematical models. This study provides descriptive morphological and biomechanical information on asymptomatic subjects. Our analyses suggest that sagittal spine balance and anatomic curvature influence postural loading and load balance of the intervertebral disc in healthy male and female subjects. Specifically, the model predicted altered and increased loads as a result of variances in the ratio of distal lumbar lordosis to total lumbar lordosis, lumbar lordosis to thoracic kyphosis, and sagittal plane translations of the cervical and thoracic regions relative to the hip axis and sacrum. These deviations might prove to be undesirable for optimum spinal structure and function. We speculate that much of this variability is related to rotation and translation displacements in the thorax and head, which may be coupled to the variations in sagittal alignment observed in this and previous studies.

Acknowledgments

The authors would like to thank the following funding agencies for their support of this research: Chiropractic Biophysics NonProfit, Inc. and the Foundation for the Advancement of Chiropractic Education. Statistical support provided by Burt Holland is also greatly appreciated.

References

[1] Harrison DD, Cailliet R, Janik TJ, Troyanovich SJ, Harrison DE, Holland B. Elliptical modeling of the sagittal lumbar lordosis and segmental rotation angles as a method to discriminate between normal and low back pain subjects. J Spinal Disord 1998;11:430–9.

[2] Steinberg EL, Luger E, Arbel R, Menachem A, Dekel S. A comparative roentgenographic analysis of the lumbar spine in male army recruits with and without lower back pain. Clin Radiol 2003;58:985–9.

[3] Schlegel JD, Smith JA, Schleusener RL. Lumbar motion segment pathology adjacent to thoracolumbar, lumbar, and lumbosacral fusions. Spine 1996;21:970–81.
[4] Kumar MN, Baklanov A, Chopin D. Correlation between sagittal plane changes and adjacent segment degeneration following lumbar spine fusion. Eur Spine J 2001;10:314–9.
[5] Umehara S, Zindrick MR, Patwardhan AG, et al. The biomechanical effect of postoperative hypolordosis in instrumented lumbar fusion on instrumented and adjacent spinal segments. Spine 2000;25:1617–24.
[6] Akamaru T, Kawahara N, Tim YS, et al. Adjacent segment motion after a simulated lumbar fusion in different sagittal alignments: a biomechanical analysis. Spine 2003;28:1560–6.
[7] Oda I, Cunningham BW, Buckley RA, et al. Does spinal kyphotic deformity influence the biomechanical characteristics of the adjacent motion segments? An in vivo animal model. Spine 1999;24:2139–46.
[8] Fukuyama S, Nakamura T, Ikeda T, Takagi K. The effect of mechanical stress on hypertrophy of the lumbar ligamentum flavum. J Spinal Disord 1995;8:126–30.
[9] Nathan M, Pope MH, Grobler LJ. Osteophyte formation in the vertebral column: a review of the etiologic factors–Part II. Contemp Orthop 1994;29:113–9.
[10] Deacon P, Flood BM, Dickson RA. Idiopathic scoliosis in three dimensions: a radiographic and morphometric analysis. J Bone Joint Surg Br 1984;66:509–12.
[11] Dickson RA. The aetiology of spinal deformities. Lancet 1988;1: 1151–5.
[12] Wenger DR, Frick SL. Scheuermann kyphosis. Spine 1999;24:2630–9.
[13] Culham EG, Jimenez HA, King CE. Thoracic kyphosis, rib mobility, and lung volumes in normal women and women with osteoporosis. Spine 1994;19:1250–5.
[14] Abdel-Hamid OA, Bassiouni H, Koutri R, Nijs J, Geusens P, Dequeker J. Aging of the thoracic spine: distinction between wedging in osteoarthritis and fracture in osteoporosis: a cross-sectional and longitudinal study. Bone 1994;15:437–42.
[15] Lauerman WC, Platenberg RC, Cain JE, Deeney VF. Age-related disk degeneration: preliminary report of a naturally occurring baboon model. J Spinal Disord 1992;5:170–4.
[16] Keller TS, Harrison DE, Colloca CJ, Harrison DD, Janik TJ. Prediction of osteoporotic spinal deformity. Spine 2003;28:455–62.
[17] Antoniades SB, Hammerberg KW, Dewald RL. Sagittal plane configuration of the sacrum in spondylolisthesis. Spine 2000;25:1085–91.
[18] Voutsinas SA, MacEwen GD. Sagittal profiles of the spine. Clin Orthop 1986;210:235–42.
[19] Repanti M, Korovessis PG, Stamatakis MV, Spastris P, Kosti P. Evolution of disc degeneration in lumbar spine: a comparative histological study between herniated and postmortem retrieved disc specimens. J Spinal Disord 1998;11:41–5.
[20] Vedantam R, Lenke LG, Keeney JA, Bridwell KH. Comparison of standing sagittal spinal alignment in asymptomatic adolescents and adults. Spine 1998;23:211–5.
[21] Gelb DE, Lenke LG, Bridwell KH, Blanke K, McEnery KW. An analysis of sagittal spinal alignment in 100 asymptomatic middle and older aged volunteers. Spine 1995;20:1351–8.
[22] Jackson RP, Kanemura T, Kawakami N, Hales C. Lumbopelvic lordosis and pelvic balance on repeated standing lateral radiographs of adult volunteers and untreated patients with constant low back pain. Spine 2000;25:575–86.
[23] Rajnics P, Pomero V, Templier A, Lavaste F, Illes T. Computer-assisted assessment of spinal sagittal plane radiographs. J Spinal Disord 2001; 14:135–42.
[24] Janik TJ, Harrison DD, Cailliet R, Troyanovich SJ, Harrison DE. Can the sagittal lumbar curvature be closely approximated by an ellipse? J Orthop Res 1998;16:766–70.
[25] Harrison DE, Janik TJ, Harrison DD, Cailliet R, Harmon SF. Can the thoracic kyphosis be modeled with a simple geometric shape?: the results of circular and elliptical modeling in 80 asymptomatic patients. J Spinal Disord Tech 2002;15:213–20.
[26] Harrison DD, Harrison DE, Janik TJ, Cailliet R, Haas J. Do alterations in vertebral and disc dimensions affect an elliptical model of thoracic kyphosis? Spine 2003;28:463–9.
[27] Kostuik JP, Hall BB. Spinal fusions to the sacrum in adults with scoliosis. Spine 1983;8:489–500.
[28] Frymoyer JW, Newberg A, Pope MH, Wilder DG, Clements J, MacPherson B. Spine radiographs in patients with low-back pain: an epidemiological study in men. J Bone Joint Surg [Am] 1984;66: 1048–55.
[29] Jackson RP, McManus AC. Radiographic analysis of sagittal plane alignment and balance in standing volunteers and patients with low back pain matched for age, sex, and size. A prospective controlled clinical study. Spine 1994;19:1611–8.
[30] Harrison DD, Colloca CJ, Troyanovich SJ, Harrison DE. Torque misuse revisited. J Manipulative Physiol Ther 1998;21:649–55.
[31] Korovessis P, Dimas A, Iliopoulos P, Lambiris E. Correlative analysis of lateral vertebral radiographic variables and medical outcomes study short-form health survey: a comparative study in asymptomatic volunteers versus patients with low back pain. J Spinal Disord Tech 2002; 15:384–90.
[32] Adams MA, Bogduk N, Burton K, Dolan P. The biomechanics of back pain. Edinburgh: Churchill Livingstone; 2002. p. 107–9.
[33] Gracovetsky S, Farfan H. The optimum spine. Spine 1986;11:543–73.
[34] Farfan HF. Form and function of the musculoskeletal system as revealed by mathematical analysis of the lumbar spine. An essay. Spine 1995;20:1462–74.
[35] Singer KP, Edmondston SJ, Day RE, Breidahl WH. Computer-assisted curvature assessment and Cobb angle determination of the thoracic kyphosis: an in vivo and in vitro comparison. Spine 1994;19:1381–4.
[36] Panjabi M, Abumi K, Duranceau J, Oxland T. Spinal stability and intersegmental muscle forces: a biomechanical model. Spine 1989;14: 194–200.
[37] Cholewicki J, Crisco JJ III, Oxland TR, Yamamoto I, Panjabi MM. Effects of posture and structure on three-dimensional coupled rotations in the lumbar spine: a biomechanical analysis. Spine 1996;21:2421–8.
[38] Kiefer A, Shirazi-Adl A, Parnianpour M. Synergy of the human spine in neutral postures. Eur Spine J 1998;7:471–9.
[39] Harrison DE, Harrison DD, Cailliet R, Troyanovich SJ, Janik TJ, Holland B. Cobb method or Harrison posterior tangent method: which to choose for lateral cervical radiographic analysis. Spine 2000;25: 2072–8.
[40] Harrison DE, Cailliet R, Harrison DD, Janik TJ, Holland B. Reliability of centroid, Cobb, and Harrison posterior tangent methods: which to choose for analysis of thoracic kyphosis. Spine 2001;26:E227–34.
[41] Harrison DE, Harrison DD, Cailliet R, Janik TJ, Holland B. Radiographic analysis of lumbar lordosis: centroid, Cobb, TRALL, and Harrison posterior tangent methods. Spine 2001;26:E235–42.
[42] Nagurka ML, Hayes WC. An interactive graphics package for calculating cross-sectional properties of complex shapes. J Biomech 1980;13: 59–64.
[43] Keller TS, Nathan M. Height change caused by creep in intervertebral discs: a sagittal plane model. J Spinal Disord 1999;12:313–24.
[44] Ruff S. Brief acceleration: less than one second. Ger Aviat Med World War II 1950;1:584–97.
[45] Crisco JJ, Panjabi MM. The intersegmental and multisegmental muscles of the lumbar spine: a biomechanical model comparing lateral stabilizing potential. Spine 1991;16:793–9.
[46] Dulhunty JA. Anthropometrical and mechanical considerations in determining normal parameters for the sagittal lumbar spine. J Manipulative Physiol Ther 1997;20:92–102.
[47] Granata KP, Wilson SE. Trunk posture and spinal stability. Clin Biomech 2001;16:650–9.
[48] Kiefer A, Shirazi-Adl A, Parnianpour M. Stability of the human spine in neutral postures. Eur Spine J 1997;6:45–53.
[49] Lavaste F, Skalli W, Robin S, Roy-Camille R, Mazel C. Three-dimensional geometrical and mechanical modelling of the lumbar spine. J Biomech 1992;25:1153–64.

[50] Shirazi-Adl A, Parnianpour M. Role of posture in mechanics of the lumbar spine in compression. J Spinal Disord 1996;9:277–86.
[51] Shirazi-Adl A, Parnianpour M. Effect of changes in lordosis on mechanics of the lumbar spine-lumbar curvature in lifting. J Spinal Disord 1999;12:436–47.
[52] Chen YL. Geometric measurements of the lumbar spine in Chinese men during trunk flexion. Spine 1999;24:666–9.
[53] George SZ, Hicks GE, Nevitt MA, Cauley JA, Vogt MT. The relationship between lumbar lordosis and radiologic variables and lumbar lordosis and clinical variables in elderly, African-American women. J Spinal Disord Tech 2003;16:200–6.
[54] Korovessis PG, Stamatakis MV, Baikousis AG. Reciprocal angulation of vertebral bodies in the sagittal plane in an asymptomatic Greek population. Spine 1998;23:700–4.
[55] Jackson RP, Peterson MD, McManus AC, Hales C. Compensatory spinopelvic balance over the hip axis and better reliability in measuring lordosis to the pelvic radius on standing lateral radiographs of adult volunteers and patients. Spine 1998;23:1750–67.
[56] Jackson RP, Hales C. Congruent spinopelvic alignment on standing lateral radiographs of adult volunteers. Spine 2000;25:2808–15.
[57] Hammerberg EM, Wood KB. Sagittal profile of the elderly. J Spinal Disord Tech 2003;16:44–50.
[58] Shirazi-Adl A, Parnianpour M. Load-bearing and stress analysis of the human spine under a novel wrapping compression loading. Clin Biomech 2000;15:718–25.
[59] Goupille P, Jayson MI, Valat JP, Freemont AJ. Matrix metalloproteinases: the clue to intervertebral disc degeneration? Spine 1998;23:1612–26.
[60] Weiler C, Nerlich AG, Zipperer J, Bachmeier BE, Boos N. 2002 SSE Award Competition in Basic Science: expression of major matrix metalloproteinases is associated with intervertebral disc degradation and resorption. Eur Spine J 2002;11:308–20.
[61] Rajnics P, Templier A, Skalli W, Lavaste F, Illes T. The association of sagittal spinal and pelvic parameters in asymptomatic persons and patients with isthmic spondylolisthesis. J Spinal Disord Tech 2002;15:24–30.
[62] Kawakami M, Tamaki T, Ando M, Yamada H, Hashizume H, Yoshida M. Lumbar sagittal balance influences the clinical outcome after decompression and posterolateral spinal fusion for degenerative lumbar spondylolisthesis. Spine 2002;27:59–64.
[63] Harrison DE, Cailliet R, Harrison DD, Janik TJ. How do anterior/posterior translations of the thoracic cage affect the sagittal lumbar spine, pelvic tilt, and thoracic kyphosis? Eur Spine J 2002;11:287–93.
[64] Harrison DE, Jones EW, Janik TJ, Harrison DD. Evaluation of axial and flexural stresses in the vertebral body cortex and trabecular bone in lordosis and two sagittal cervical translation configurations with an elliptical shell model. J Manipulative Physiol Ther 2002;25:391–401.
[65] Manns RA, Haddaway MJ, McCall IW, Cassar PV, Davie MW. The relative contribution of disc and vertebral morphometry to the angle of kyphosis in asymptomatic subjects. Clin Radiol 1996;51:258–62.
[66] Loder RT. Profiles of the cervical, thoracic, and lumbosacral spine in children and adolescents with lumbosacral spondylolisthesis. J Spinal Disord 2001;14:465–71.
[67] Itoi E. Roentgenographic analysis of posture in spinal osteoporotics. Spine 1991;16:750–6.
[68] Harrison DE, Colloca CJ, Harrison DD, Janik TJ, Haas JW, Keller TS. Anterior thoracic posture increases lumbar intervertebral disc loading. Eur Spine J (in press). [Published on-line: DOI: 10.1007/s00586-004-0734-0].
[69] McGill SM, Norman RW. Partitioning of the L4–L5 dynamic moment into disc, ligamentous, and muscular components during lifting. Spine 1986;11:666–77.
[70] Nussbaum MA, Chaffin DB. Development and evaluation of a scalable and deformable geometric model of the human torso. Clin Biomech 1996;11:25–34.
[71] Pearsall DJ, Reid JG, Livingston LA. Segmental inertia parameters of the human trunk as determined from computer tomography. Ann Biomed Eng 1996;24:198–210.
[72] Falhallah FA, Marras WS, Parnianpour M. An assessment of complex loads during dynamic lifting tasks. Spine 1998;23:706–16.
[73] Davis JR, Mirka GA. Transverse-contour modeling of trunk muscle-distributed forces and spinal loads during lifting and twisting. Spine 2000;25:180–9.